# Deliverable

# H2020 COMPET-05-2015 project
# "Small Bodies: Near And Far (SBNAF)"

**Topic**: COMPET-05-2015 - Scientific exploitation of astrophysics, comets, and planetary data
**Project Title**: Small Bodies Near and Far (SBNAF)
**Proposal No**: 687378 - SBNAF - RIA
**Duration**: Apr 1, 2016 - Mar 31, 2019

| WP | WP6, Synergies from ground and space |
|---|---|
| Del.No | D6.1 |
| Title | Occultation vs. thermal tools |
| Lead Beneficiary | UAM |
| Nature | Report |
| Dissemination Level | Public |
| Est. Del. Date | 31 January 2017 |
| Version | 1.0 |
| Date | February 1, 2017 |
| Lead Author | Alí-Lagoa, V.; MPE (vali@mpe.mpg.de) |

Objectives of WP: To combine observational data from space and ground, from remote, disk-integrated data and disk-resolved data from interplanetary missions to obtain (validated) high-quality model solutions for a wide range of applications: improvement of the scientific understanding, answering key questions for the reconstruction of minor body properties, calibration aspects, support for Gaia density determination, Hayabusa-2 target characterization and operational support, tools and methods for applications to large object samples.

# Description of deliverable

Establishment of tool to translate occultation constraint into possible 3-D object properties for testing against thermal measurements.

# Contents

# 1  Introduction

Small bodies in the Solar System constitute an heterogeneous population, so we need to characterise them in large numbers if we want to understand their nature and infer information about their past and evolution. Determining their size, their most basic physical property, is not trivial since the vast majority of objects are too small to be resolved remotely by typical observing techniques. It has been only (relatively) recently that we have managed to estimate small body sizes in great quantities by means of asteroid thermal models applied to large thermal infrared data sets afforded by space-based surveys. These are called "radiometric diameters".

Radiometric diameters or sizes are indirect, model-dependent estimates that rely on a number of simplifying assumptions, however. Radar observations, adaptive optics, or stellar occultations constitute more "direct" methods of estimating sizes, but the amount of objects amenable to these techniques is much more limited than radiometry, for different reasons in each case. In spite of this, obtaining size determinations by these methods provides invaluable independent estimates against which to test the thermal (and thermophysical) model predictions.

Conversely, these more direct methods still have their own limitations, as it will be illustrated in this deliverable for the case of stellar occultations. Our aim here is to enumerate and discuss in a unified document –which is lacking in the specialised literature– several cases relevant for our SBNAF targets in which modelling of thermal infrared/sub-millimetre data can complement stellar occultation observations in order to maximise our knowledge. This will lay out some optimal guidelines to follow in each particular case as new data are collected. The different cases arise from the different kind of information probed by these two observational techniques, the distinct physical characteristics of the two type of small bodies observable through occultations, main belt asteroids and trans-Neptunian objects, and what other data (light curves, shapes, rotational and thermal properties, densities, . . .) may also be available for the target.

This document will be made publicly available in the SBNAF public website[1], so we will also provide brief notes on stellar occultations and thermal and thermophysical models in Secs. 2.1 and 2.2 to make it self-contained. In Sec. 3 we provide a summary chart showing which limitations and strengths of occultations and thermal tools complement each other. In Secs. 4 and 5 we enumerate the cases that we can expect to tackle in the framework of our project for main-belt asteroids (MBAs) and trans-Neptunian objects (TNOs) separately. Section 6 offers some concluding remarks.

---

[1]http://www.mpe.mpg.de/ tmueller/sbnaf/

## 2 Brief introductory notes

### 2.1 Stellar occulations

An occultation of a star by an object takes place when said object crosses the observer's line of sight towards the star. As a consequence, the brightness of the star diminishes during the event. Any extended object will produce a shadow whose projection on the Earth retains its size because the stars are effectively at infinity (a schematic view is given in the left panel of Fig. 1). Thus, if several observers at different latitudes measure the duration of the dimming[2] at their locations accurately, the shape of the object can be reconstructed by projecting these recorded times on the plane of the sky, which produces segments called chords. The right panel of Fig.1 (taken from Bartczak et al. 2014a) shows the impressive set of chords obtained by Colas et al. (2012) for the binary asteroid (90) Antiope and its companion. The silhouettes are the best-fitting, non-convex shape model derived by Bartczak et al. (2014a) from light-curve (LC) inversion using the SAGE algorithm.
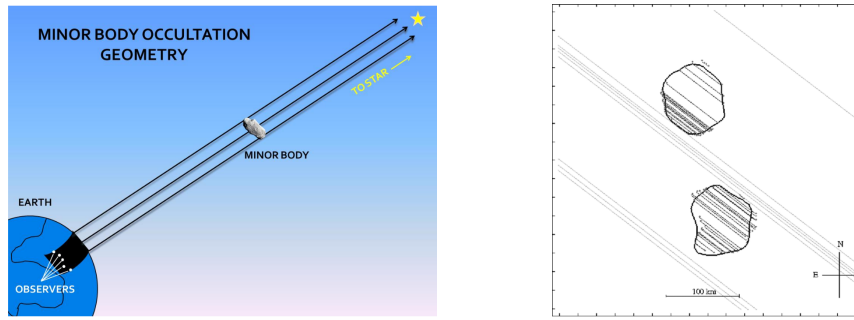


Figure 1: Left: Schematic of a stellar occultation taken from Santos-Sanz et al. (2016). Right: example of a chords and best-fitting silhouettes for binary asteroid (90) Antiope taken from Bartczak et al. (2014a).

Occultations may allow one to reconstruct the shapes of irregular objects to a degree of precision unattainable from other ground-based techniques. Even the presence of thin atmospheres or rings have been revealed for some trans-Neptunian objects and Centaurs (see e.g. Sicardy et al. 2011; Ortiz et al. 2012; Braga-Ribas et al. 2014). These, and other examples like (90) Antiope, are extremely optimal cases, however. Even though observing occultations does not require sophisticated instrumentation and dedicated amateur observers actually contribute the most to the acquisition of data[3], there are a number of inescapable difficulties and associated uncertainties (for a review, see Durech et al. 2015, and references therein). The critical one is the absolute timing of the events because, together with the geographical position –much more reliable thanks to the Global Positioning System or GPS–, it determines the extent and positions of the chords on the plane of the sky projection. Durech et al. give the example of an asteroid at 1.5 au from the observer, moving at 10 arc sec/hour: an error of 50 ms in the chord timing translates into an error of 300 m. Furthermore, it is far from easy to ensure successful shadow predictions in order to plan observations in well-

---

[2]These range from a few seconds to ~100 s. The duration is determined by the ratio of the apparent diameter (arc seconds) to the apparent motion on the object (arc seconds/unit time). For instance, a hypothetical 1500-km wide TNO at 50 au from the Earth subtends about 4 arc seconds. If it moved at 2 arc sec/hour, we would obtain a duration of ~70 seconds for a central occultation.

[3]Visit, for instance, http://www.euraster.net.

distributed locations due to the uncertainties in the positions of the stars and the small bodies. Thus, in more frequent, less optimal cases, one can fit ellipsoids to a few chords, get a minimum estimate of the object's extent from at least one chord.

Interestingly, the publication of the complete Gaia catalogue will improve the astrometry of main-belt asteroid orbits by two orders of magnitude. This has led to the prospect that the full census of asteroid sizes down to 20 km determined from occultations could be achieved within a few years (Tanga & Delbo 2007). The case is not so encouraging for TNOs even in the "post-Gaia" era, since their orbital periods are so long that their orbits can only be estimated from short arcs, which keeps the uncertainties high. Table 1 in Santos-Sanz et al. (2016) includes a set of dates and locations of recent stellar occultations by TNOs.

## 2.2 Thermal and thermophysical models

*Radiometry* refers to the determination of the radius of the small body by fitting thermal emission models to observed thermal flux densities. The first applications of these techniques date back to the 1970's (for a recent review, see Delbo et al. 2015). The basic principle underlying these models is the conservation of energy, and more sophisticated physics can be added depending on the physical information available for the targets, as we will briefly mention below.

In a nutshell, the warmer a body is, the higher its emitted flux needs to be in order to stay in thermal equilibrium. Take an infinitely flat triangular plate or facet, for instance. In general, the closer it is to the sun, the higher its temperature is expected to be, but it actually depends on the orientation of the flat surface with respect to the sunward direction. Furthermore, materials do not completely absorb or reflect all incident energy, so those with high reflectances or albedos will not warm up as much as low albedo ones. Considering that a body can be represented as a collection of facets (a polyhedron; see Fig. 2) oriented in space and located at a particular distance from the sun, its particular shape and orientation in space as well as the albedo of its constituting materials will determine the instantaneous surface temperature distribution, because sunlight reaches different surface elements at different angles. This will then determine the disc-integrated thermal flux density measured by an observer, along with the target's size and the particular part of the body that is visible from the observer's position.
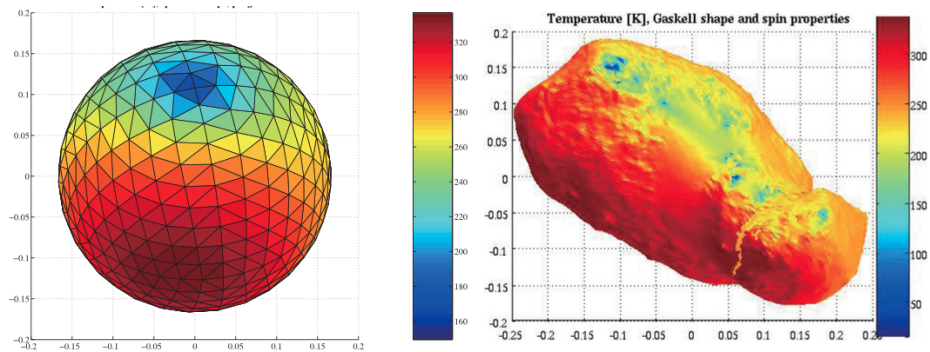


Figure 2: Two shape models with facets coloured as a function of temperature computed from thermophysical models (taken from Müller et al. 2014). Left panel: spherical shape. Right panel: Itokawa's shape based on images taken by the Hayabusa mission (Demura et al. 2006). Note that, unlike what is shown in the left panel, the NEATM temperature distribution would fall steadily from the hottest facet (the so-called subsolar point) to an idealised 0 K at the terminator and all the non-illuminated facets.

4

Once the orbit of a small body is determined, the relative positions of the sun, the body and the observer at the times of observation are known and it is then possible to find sets of values of model parameters (such as size) that best fit the thermal data. When there is no available shape information for the target, models assume non-rotating spherical bodies made of a non-conducting material. Since these work with spheres, the word "size", used interchangeably with diameter, actually refers to the diameter of the sphere with the same projected cross-sectional area. These are usually called "thermal models" and, while there are different types that make different simplifying assumptions, the "near-Earth thermal model" (NEATM) of Harris (1998) is currently most widely used, as it is not only applicable to NEAs. On the other hand, if the shape and rotational properties of the object are known, we can also model instantaneous surface temperatures accounting for the heat conductivity of the material as well as surface roughness (Fig. 2). These are typically called "thermophysical models" (TPM). In some circumstances, even if the shape is not available, one can use spheres instead and still obtain good estimates for the thermal/thermophysical properties of the target (Müller et al. 2014).

## 3 Occultations versus thermal tools complementarity

The complementary aspects of the knowledge about our SBNAF targets that we can gain from these two techniques can be conveniently summarised by comparing in a one-to-one fashion their respective limitations (L) and strengths (S):

| Occultations | Thermal/Thermophysical tools |
|---|---|
| S: Accurate chords provide precise, direct constraints for spatial extent and shape features with a few km accuracy | L: Even high-quality data can produce model-dependent results. Thermal model diameters can be accurate to within 10%. TPM ~5%, but well-sampled data in the visible needed to infer reliable shapes and spin-pole orientations |
| L: Two-dimensional, instantaneous snapshots. No information about rotation or volume or surface physical nature | S: Modelling of several measurements can capture three-dimensional information, as well as surface thermal properties and rotation-related information |
| L: Hard to predict with success. Typically few chords obtained. Errors in timing strongly affect inferred sizes. Not possible to reproduce events, low probability of occulting other stars in near future | S: Several multi-epoch, multi-wavelength, and multi-phase observations can help average out biases and model-related errors. Measurement repetitions are possible |
| S: Sensitive to satellites, rings, and atmospheres | L: TPMs do not include radiative transfer physics required to model atmospheres; thermal IR/sub-mm data are insensitive to rings (depending on grain size). |

# 4 Main-belt asteroids

Throughout its journey around the Sun, it is possible to observe (over the course of several years) different aspects of an asteroid whose orbit has a sufficiently high inclination with respect to the ecliptic and infer a unique solution from LC inversion techniques. Otherwise, for asteroids whose orbital inclinations are low, two or more equally well-fitting solutions are obtained (Magnusson 1986; Michalowski 1993; Kaasalainen et al. 2002, and references therein). While both occultations and thermophysical models can provide an absolute scale for the LC-inverted shapes and remove the degeneracy, the circumstances in which this is the case and the accuracy of these constraints can differ noticeably; cases relevant for our SBNAF targets are enumerated in the following sections.

Thermophysical models are especially well suited (but not limited; e.g. Delbo' & Tanga 2009), to identify which one among two possible spin-pole solutions with opposite senses of rotation better reproduces thermal IR data (e.g., Müller 2002; Müller et al. 2012, 2013). This is due to the effects of thermal inertia, which results in lower (higher) morning (evening) temperatures than those for the zero-thermal inertia case[4] (see the review by Delbo et al. 2015). However, this effect is only sufficiently pronounced if the period of rotation is not too short or too long (say, > 2 h or <30 h), and the spin axis is not too close to the ecliptic plane, as the emitted fluxes of pole-on rotators will not evidence a strong thermal lag regardless of their thermal inertia and period of rotation. The reason is that the illumination of the surface elements, and hence their temperature, does not change enough.

A good set of occultation chords can also help eliminate one of the ambiguous solutions (hopefully not both) from LC inversion as long as the silhouette is not too spherical. An illustrative example taken from Durech et al. (2011), is shown in Fig. 3. It must be mentioned, though, that combining available occultation and optical data was not always sufficient to discard ambiguous solutions in the Durech et al. work. Likewise, although ongoing efforts to model optical and thermal data simultaneously to infer shapes from inversion have manage to provide unique solutions (Durech, private communication), this is not always the case (Durech et al. 2016; Müller et al. 2016).
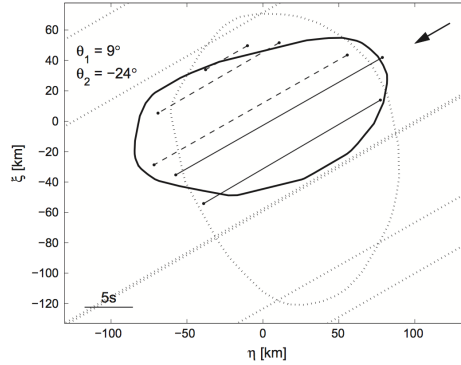


Figure 3: Example taken from Durech et al. (2011) of the two ambiguous solutions of asteroid (471) Papagena obtained from LC inversion. When they were scaled to fit occultation chords, one of them was clearly not compatible with the non-detections (dotted lines).

---

[4]This is something we can perceive on Earth: the temperatures of fine sand are cooler in the early mornings and evenings and the warmest at noon; on the other hand, big boulders stay warm for a longer time during the evening and cooler in the mornings, reaching their peak temperatures some time after noon.

In the pre-Gaia era (see Sec. 2.1), MBAs observed by programmed occultations will usually be relatively large (>50 km) ones. SBNAF targets will likely have some available photometry for LC inversion or it may be possible to acquire it. Thus, we will tend to work with targets in Case 1, but those from Case 2 may also be relevant when it is not possible to derive a reliable shape.

## 4.1 Case 1: available rotational properties and shape

A good set of chords can help ensure the accuracy of a shape and spin pole inferred from LC inversion, or indeed be used as a constraint to model the optical data (see Durech et al. 2015, for a review). A great example is given by Bartczak et al. (2014b), who used the SAGE algorithm (Bartczak et al. 2014a) to infer a non-convex shape of MBA (9) Metis from LC inversion. Figure 4 shows the silhouette of the convex and non-convex shape models projected along a set of occultation chords. The SAGE model nicely reproduces the concavities evidenced by the chords.
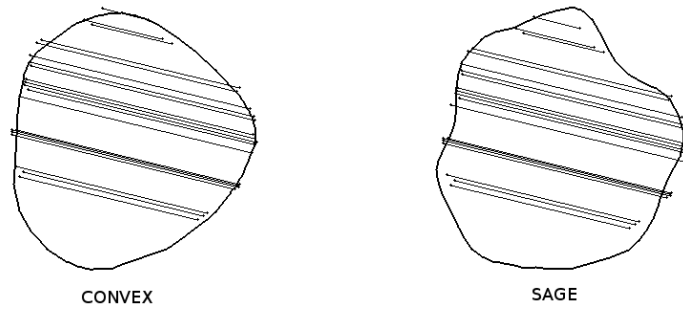


CONVEX                    SAGE

Figure 4: Occultation chords of main-belt asteroid (9) Metis and projected silhouettes of a convex and non-convex shape models derived from LC inversion. The non-convex model obtained with the SAGE algorithm (Bartczak et al. 2014a) correctly reproduces the concavities.

This is the best conceivable scenario to study the thermophysical properties of an object based on data obtained remotely, since the shape can be confidently given an absolute scale, which will remove one of the free parameters of the TPM.

## 4.2 Case 2: no shape available

Optical data can provide reasonable estimates of the period of rotation even in cases when obtaining shapes from LC inversion is not possible, and recent efforts also benefit from thermal light curves to improve period determinations as well (Durech et al. 2016; Müller et al. 2016). In these cases, thermal data covering a sufficient fraction of the rotational period can be modelled to infer radiometric diameters that reasonably represent the volume of the object. This is something that occultations cannot ensure for irregular or elongated objects, since the silhouette may happen to capture one of the extreme aspects of the shape. Still, for the largest (and expectedly more regularly-shaped) main belt asteroids in our target list (numbered 1, 2, 3, 4, 6, 7, 8, 9, 10, 14, 16, 18, 19, 20, and 21), thermal modelling of AKARI data (Usui et al. 2011) yields diameters that correlate very well with occultation ones, as shown in Fig. 5.

Thus, if a good occultation-based diameter is also available to give the model sphere an absolute scale, thermophysical models using spheres can constrain the sense of rotation if the thermal data are obtained at two epochs, one pre-opposition, the other post-opposition (e.g. Table 2 in Müller 2002),
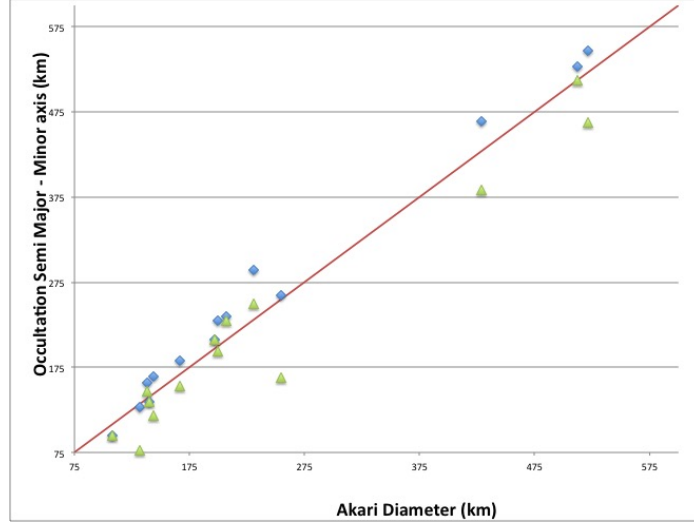
Figure 5: Occultation major axis (blue) and minor axis (green) versus AKARI-derived radiometric diameters (Usui et al. 2011) of some of the largest SBNAF targets (see text). The occultation sizes spread reasonably evenly around the line $y = x$ (red), suggesting these radiometric sizes are not affected by significant model-dependent biases, which is expected given these objects are more likely to verify the idealised assumptions of the NEATM: they are large, more regularly-shaped objects covered by an insulating layer of fine regolith and whose poles are oriented far from the ecliptic.

and possibly even a reasonable guess for the direction of the pole. This applies if the (unknown) obliquity is not too high, the thermal inertia is not very low, and the rotation period is not too long or too short.

# 5 Trans-Neptunian objects

TNOs pose a much greater observational challenge in many aspects. With orbital periods on the order of ~100 years, the apparent motion of these objects is so slow that it has not been possible to observe them at different aspect angles. This makes LC inversion unsuitable to infer TNO shapes, not to mention that albedo variegations are not infrequent (see e.g. the review by Stansberry et al. 2008). Owing to their long heliocentric distances and ensuing faintness, obtaining good thermal IR data is significantly more difficult in the case of TNOs. Occultations are also very difficult to predict with accuracy (see Sec. 2.1) because of the higher uncertainties in their orbits, so the number of TNOs for which several chords have been obtained from single occultation events is limited to five objects (see Table 1 in Schindler et al. 2016, and references therein).

In spite of these difficulties, scientific exploitation is still possible in some cases thanks to the fact that optical observations, by means of which these objects are discovered, suffer from a strong observational bias against small TNOs (< 100 km). Hence, the majority are in hydrostatic equilibrium, in consistency with their small light-curve amplitudes (Duffard et al. 2009; Thirouin et al. 2010). This bias constitutes an important constraint in itself: by assuming hydrostatic equilibrium, one can fit ellipsoidal figures to optical light curves (e.g. Lacerda & Jewitt 2007) and/or occultation chords (Schindler et al. 2016, and references therein). A large percentage of the objects have peak-to-peak light-curve amplitudes smaller than 0.15 magnitudes (Duffard et al. 2009; Santos-Sanz 2009; Thi-
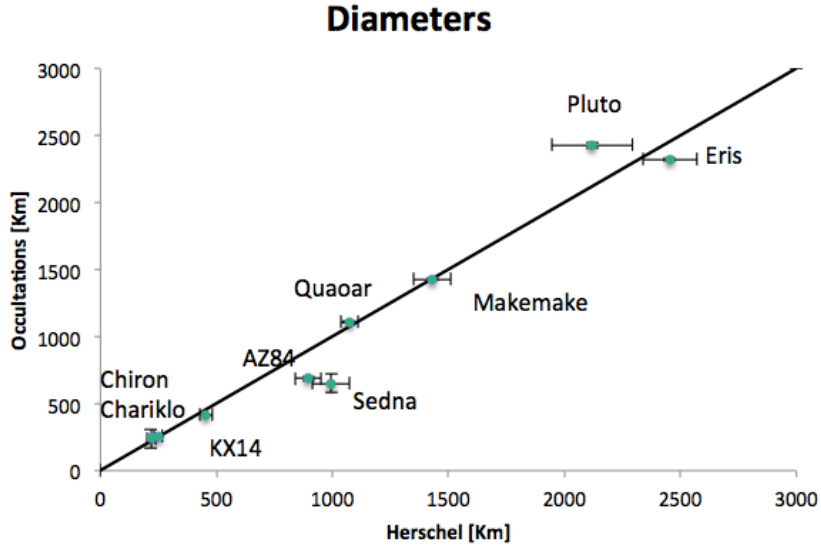
8

**Diameters**



Figure 6: Set of occultation diameters of TNOs and large centaurs versus their radiometric counterparts derived from Herschel. The black line is $y = x$.

rouin et al. 2010), suggesting they are oblate Maclaurin spheroids (ellipsoids with semi-major axes $c < a = b$). Fast rotators, on the other hand, are Jacobi ellipsoids ($a \neq b \neq c$), and hence show higher light-curve amplitudes unless they are observed pole-on. Moreover, these shapes, Maclaurin spheroids and Jacobi ellipsoids, produce single-peaked or double-peaked light curves, respectively (see Thirouin 2013, for a review).

The usual approach to fit the occultation data is to find the best-fitting shape by $\chi^2$ minimisation taking into account the timing errors, which influence the length of the chords[5]. Occultation-based and radiometric diameters often correlate remarkably well, suggesting there are no major systematic biases at play (Fig. 6). An important factor is that, with relatively regular shapes and low thermal inertias, currently observable TNOs do not deviate much from two key simplifying assumptions of thermals models (see Sec. 2.2). There are on the order of ∼100 radiometric diameters inferred mostly from space-based facilities like Spitzer and/or Herschel (Stansberry et al. 2008; Müller et al. 2010; Santos-Sanz et al. 2012; Lellouch et al. 2013; Duffard et al. 2014).

*Procedure for Maclaurin spheroids*

The hydrostatic equilibrium model for Maclaurin spheroids is particularly beneficial because it allows one to tackle the problem of inferring a three-dimensional shape from the two-dimensional occultation profile with a more systematic approach. It is not difficult to illustrate how the relationship between the period of rotation, $P$, and the flattening of the shape, $\epsilon = (a - c)/a$, can rule out a large portion of the space of possible parameter values even if the period of rotation is not well determined.

---

[5]Schindler et al. (2016) considered an "error in variables" problem, i.e. that the $x$ and $y$ components of the chords in the plane of the sky have uncertainties. While this resulted in larger uncertainties of the fitted parameters, their solution was very similar with the one derived from the usual $\chi^2$ method.

Basically, one can infer the true flattening $\epsilon = (a-c)/a$ based on the observed flattening $\epsilon' = (a'-c')/a'$ in an occultation (see the Supplementary Information in Sicardy et al. 2011, and references therein). Taking into account that $a' = a$, both are related by $\theta$, the angle between the rotation axis of the object and the line of sight:

$$1 - \epsilon = \frac{\sqrt{(1-\epsilon')^2 - \cos^2\theta}}{\sin\theta}. \tag{1}$$

Now, the rotation period also determines the value of $\epsilon$, so we have

$$\epsilon = f(P). \tag{2}$$

In principle, these two equations suffice to solve for $\theta$ and then find $\epsilon$, but reality is more complicated because the Maclaurin spheroid assumption requires good optical data to find reliable values of $P$ and the light curve amplitude. Furthermore, the mass needs to be known from independent measurements, most likely from the characterisation of the orbit and orbital period of a satellite. And, because the internal structure is not known, a uniform density is often assumed for Eq. 2 (Sicardy et al. 2011).

When $P$ is not available or not well constrained, additional information may come from observations of emitted fluxes, which are not so sensitive to $\epsilon'$ but to the total projected area, which can be quantified in terms of a measured equivalent radius $R_E = f(\epsilon') = f(a', c')$. The key is that there is only one value of $\epsilon'$ compatible with $R_E$, so we have

$$R_E = g(\epsilon') = g'(\theta, \epsilon) = g''(\theta, a). \tag{3}$$

One can then produce many TPM model fluxes based on different rotation periods and $\theta$ and find those that match $\epsilon'$. Then, only a subset of models with the appropriate values of $\theta$ and $P$, or equivalently, $\theta$ and $a$, will simultaneously match the independently observed $\epsilon'$ and $R_E$. To sum up, one can measure $\epsilon'$ from the occultation chords and find what pairs $\theta$ and $\epsilon$ are compatible. For each pair, there is only a possible rotation period $P$ and set of thermophysical parameters that will reproduce the values of $\epsilon'$ or, equivalently, $R_E$ (Eq. 3). Thus we are left with a set of valid solutions with certain values of $\theta$, $P$, and $a$.

## 5.1 Case 1: known rotational period

It is possible to infer the shape (more specifically, the ratio $a/c$) for Maclaurin spheroids if the rotation period is known, but a good *a priori* estimate of the density is required. For Jacobi ellipsoids, one can derive a lower limit for the density and best-fitting semi-major axes from the rotation period too, but one needs to assume the spatial orientation of the rotation axis. Occultation information coupled with modelling thermal IR/sub-mm observations may offer the missing information in both situations.

Two examples of Maclaurin spheroids whose axis of rotation are constrained by thermal IR/sub-mm data are (136472) Makemake and binary (208996) 2003 $AZ_{84}$. Ortiz et al. (2012) fitted a Maclaurin spheroid to several occultation chords of Makemake. Its optical light curve had a low amplitude, along with the fact that Makemake presented thermal data at 24 $\mu$m that were not possible to fit by TPMs without invoking strong albedo variegations (Lim et al. 2010, and references therein), suggested that it was observed pole-on. Instead of albedo variegations, Lim et al. also suggested the possible influence of a low-albedo moon to explain the 24-$\mu$m data, which was later confirmed (Parker et al. 2016).

The analysis of binary (208996) 2003 AZ$_{84}$ carried out by Santos-Sanz et al. (submitted to A&A) also combined optical and thermal light curves with constraints from occultations (Dias-Oliveira et al. 2016) and concluded that AZ$_{84}$ must be viewed close to pole-on ($\pm 30°$), too. In this case, this was implied by its small optical light-curve amplitude as well as the fact that equator-on TPMs cannot reproduce both the occultation size and Herschel/PACS fluxes simultaneously unless very unrealistic parameter values of the TPM were adopted. Thus, the availability of an occultation-based size was crucial.

## 5.2   Case 2: unknown rotational period

If the rotation period is unknown, one cannot resort to estimates of modelled equilibrium shapes. Still, if the occultation chords are sufficiently good to find an ellipsoid fit and there is thermal/sub-mm data available, the absolute scale implied by the former may help find constraints for a large set of TPM models covering reasonable values of rotational period, thermal inertia, and roughness. For instance, occultation combined with Herschel/PACS data favoured a pole-on view of TNO (229762) 2007 UK$_{126}$ (Schindler et al. 2016), since equator-on models could clearly not reproduce the sub-mm data for any reasonable set of values assumed for the thermal properties.

# 6   Outlook

In this deliverable we have collected all complementary aspects of occultation and thermal tools that we will prospectively exploit during our project. It will not only serve as a reference guideline, but it helps demonstrate how fundamental new occultation data are for SBNAF and justifies all the efforts devoted to obtaining them in addition to visible photometry. Good occultation data can ensure the reliability of non-convex shapes of MBAs derived from LC inversion or enhance the information we can obtain from modelling TNOs thermal IR/sub-mm data. Ultimately, having comprehensive information about our targets is the only way to test the quality of our current models and identify weaknesses or limitations. These will warrant the development of new tools to maximise the scientific return obtained from remote space- (IR/sub-mm) and ground-based (visible photometry and occultation) data.

# References

Bartczak, P., Michałowski, T., Santana-Ros, T., & Dudziński, G. 2014a, MNRAS, 443, 1802

Bartczak, P., Santana-Ros, T., & Michalowski, T. 2014b, in Asteroids, Comets, Meteors 2014, ed. K. Muinonen, A. Penttilä, M. Granvik, A. Virkki, G. Fedorets, O. Wilkman, & T. Kohout

Braga-Ribas, F., Sicardy, B., Ortiz, J. L., et al. 2014, Nature, 508, 72

Colas, F., Berthier, J., Vachier, F., et al. 2012, in LPI Contributions, Vol. 1667, Asteroids, Comets, Meteors 2012, 6427

Delbo, M., Mueller, M., Emery, J. P., Rozitis, B., & Capria, M. T. 2015, Asteroid Thermophysical Modeling, ed. P. Michel, F. E. DeMeo, & W. F. Bottke, 107–128

Delbo', M. & Tanga, P. 2009, Planet. Space Sci., 57, 259

Demura, H., Kobayashi, S., Nemoto, E., et al. 2006, Science, 312, 1347

Dias-Oliveira, A., Sicardy, B., Ortiz, J.-L., et al. 2016, in AAS/Division for Planetary Sciences Meeting Abstracts, Vol. 48, AAS/Division for Planetary Sciences Meeting Abstracts, 106.09

Duffard, R., Ortiz, J. L., Thirouin, A., Santos-Sanz, P., & Morales, N. 2009, A&A, 505, 1283

Duffard, R., Pinilla-Alonso, N., Santos-Sanz, P., et al. 2014, A&A, 564, A92

Durech, J., Carry, B., Delbo, M., Kaasalainen, M., & Viikinkoski, M. 2015, Asteroid Models from Multiple Data Sources, ed. P. Michel, F. E. DeMeo, & W. F. Bottke, 183–202

Durech, J., Hanuš, J., Alí-Lagoa, V. M., Delbo, M., & Oszkiewicz, D. A. 2016, in IAU Symposium, Vol. 318, IAU Symposium, ed. S. R. Chesley, A. Morbidelli, R. Jedicke, & D. Farnocchia, 170–176

Durech, J., Kaasalainen, M., Herald, D., et al. 2011, Icarus, 214, 652

Kaasalainen, M., Mottola, S., & Fulchignoni, M. 2002, Asteroids III, 139

Lacerda, P. & Jewitt, D. C. 2007, AJ, 133, 1393

Lellouch, E., Santos-Sanz, P., Lacerda, P., et al. 2013, A&A, 557, A60

Lim, T. L., Stansberry, J., Müller, T. G., et al. 2010, A&A, 518, L148

Magnusson, P. 1986, Icarus, 68, 1

Michalowski, T. 1993, Icarus, 106, 563

Müller, T. G. 2002, Meteoritics and Planetary Science, 37, 1919

Müller, T. G., Hasegawa, S., & Usui, F. 2014, PASJ, 66, 52

Müller, T. G., Lellouch, E., Stansberry, J., et al. 2010, A&A, 518, L146

Müller, T. G., Miyata, T., Kiss, C., et al. 2013, A&A, 558, A97

Müller, T. G., O'Rourke, L., Barucci, A. M., et al. 2012, A&A, 548, A36

Müller, T. G., Ďurech, J., Ishiguro, M., et al. 2016, ArXiv e-prints

Ortiz, J. L., Sicardy, B., Braga-Ribas, F., et al. 2012, Nature, 491, 566

Parker, A. H., Buie, M. W., Grundy, W. M., & Noll, K. S. 2016, ApJ, 825, L9

Santos-Sanz, P. 2009, Doctoral Dissertation (available from http://digibug.ugr.es/handle/10481/2387

Santos-Sanz, P., French, R. G., Pinilla-Alonso, N., et al. 2016, PASP, 128, 018011

Santos-Sanz, P., Lellouch, E., Fornasier, S., et al. 2012, A&A, 541, A92

Schindler, K., Wolf, J., Bardecker, J., et al. 2016, ArXiv e-prints

Sicardy, B., Ortiz, J. L., Assafin, M., et al. 2011, Nature, 478, 493

Stansberry, J., Grundy, W., Brown, M., et al. 2008, Physical Properties of Kuiper Belt and Centaur Objects: Constraints from the Spitzer Space Telescope, ed. M. A. Barucci, H. Boehnhardt, D. P. Cruikshank, A. Morbidelli, & R. Dotson, 161–179

Tanga, P. & Delbo, M. 2007, A&A, 474, 1015

Thirouin, A. 2013, Doctoral Dissertation, (available from http://hdl.handle.net/10481/30832)

Thirouin, A., Ortiz, J. L., Duffard, R., et al. 2010, A&A, 522, A93

Usui, F., Kuroda, D., Müller, T. G., et al. 2011, PASJ, 63, 1117